

Hydromagnetic natural convection flow with induced magnetic field and n^{th} order chemical reaction of a heat absorbing fluid past an impulsively moving vertical plate with ramped temperature

G. S. Seth*, S. Sarkar

Department of Applied Mathematics, Indian School of Mines, Dhanbad, India

Received January 3, 2014; Revised August 26, 2014

An investigation of the unsteady hydromagnetic natural convection flow with heat and mass transfer of a viscous, incompressible, electrically conducting and heat absorbing fluid past an impulsively moving vertical plate with ramped temperature embedded in a fluid-saturated porous medium is carried out taking induced magnetic field and n^{th} order chemical reaction into account. Governing equations along with the initial and boundary conditions are solved numerically using the Crank-Nicolson implicit finite difference scheme. The numerical solutions for fluid velocity, induced magnetic field, species concentration and fluid temperature are depicted graphically, whereas the numerical values of skin friction, Sherwood number and Nusselt number are presented in tabular form for various values of the pertinent flow parameters. In order to highlight the influence of ramped temperature distribution within the plate on the flow-field, the fluid flow past a ramped temperature plate is compared with the one past an isothermal plate. Validation of numerical results is also performed to ensure correctness of the results.

Keywords: Induced magnetic field, thermal buoyancy force, concentration buoyancy force, ramped temperature, heat absorption, n^{th} order chemical reaction.

INTRODUCTION

Natural convection flow resulting from the simultaneous action of thermal and concentration buoyancy forces occurs frequently in nature and has significant engineering applications. Atmospheric flows are driven not only by temperature differences but also by concentration differences since in nature air or water are usually contaminated by suspended particulate matter which may be present either naturally or due to industrial emissions. A comprehensive discussion on convective heat and mass transfer was made by Eckert and Drake [1] through their book "Analysis of Heat and Mass Transfer" which included all previous investigations and laid the groundwork for future research. Later, natural convection heat and mass transfer flow through a fluid saturated porous medium has been investigated by several researchers [2-5] because of its varied and wide range of industrial applications such as enhanced recovery of petroleum products and gases (e.g. CBM: coal bed methane and UCG: underground coal gasification), dispersion of chemical contaminants through water-saturated soil, solid matrix heat exchangers, desert coolers, wet bulb thermometers, packed bed reactors, underground disposal of nuclear waste, exploitation of continental geothermal reservoir, etc.

Hydromagnetic flows with heat and mass transfer in porous media have been considered extensively in recent years due to their occurrence in several engineering applications such as in boundary layer flow control, magnetic levitation and casting, filtration of liquid metals, cooling of nuclear reactors, fusion control, prevention of scaling in heat exchangers, etc. Moreover, the study of unsteady hydromagnetic flows is significant from practical point of view because fluid transients may be expected at the start-up time of many industrial processes and devices, *viz.* MHD power generators, MHD pumps, MHD accelerators, MHD flow-meters, controlled thermonuclear reactors, etc. Keeping in view the importance of such study, several researchers [6-10] have investigated unsteady hydromagnetic natural convection heat and mass transfer flow of a viscous, incompressible and electrically conducting fluid past a flat plate embedded in a fluid-saturated porous medium. It is noticed that there may be significant temperature difference between ambient fluid and surface of the solid in a number of fluid flow problems of physical interest, *viz.* fluids undergoing exothermic and/or endothermic chemical reaction, heat removal from nuclear fuel debris, underground disposal of radioactive waste material, storage of food stuffs, dissociating fluids in packed bed reactors, etc. Therefore, it is suitable to consider temperature dependent heat source and/or sink which may have strong influence on heat transfer characteristics. Keeping in view the importance of such study,

* To whom all correspondence should be sent:
E-mail: gsseth.ism@gmail.com

Chamkha and Khaled [11] investigated hydromagnetic natural convection heat and mass transfer flow past a permeable vertical plate embedded in a fluid-saturated porous medium in the presence of heat generation or absorption. Kamel [12] considered unsteady hydromagnetic natural convection flow due to heat and mass transfer through a porous medium bounded by an infinite vertical porous plate with temperature-dependent heat sources/sinks. Chamkha [13] analyzed unsteady hydromagnetic natural convection heat and mass transfer flow past a semi-infinite vertical moving plate with heat absorption.

In chemical and hydrometallurgical industries, the production of polymers, ceramics and glassware often involve processes that require combined heat and mass transfer over surfaces with different geometries where diffusing species can be generated or absorbed due to some kind of chemical reaction with the ambient fluid and can greatly affect the flow characteristics, as well as the quality of the final product. However, the effect of a chemical reaction significantly depends on its order and whether the reaction is heterogeneous or homogenous. In general, a reaction is said to be of n^{th} order if the rate of reaction is proportional to the n^{th} power of concentration itself. Chemical reactions are said to be heterogeneous or homogenous depending on whether they occur at an interface or as a single phase volume reaction. A homogenous reaction occurs uniformly throughout the given phase, whereas a heterogeneous reaction takes place in a restricted region or within the boundary of a phase. Chambre and Young [14] were among the initial investigators to study the diffusion of a chemically reactive species in a laminar boundary layer flow over a flat plate. Das *et al.* [15] studied the effect of homogenous first order chemical reaction on the flow of an impulsively started infinite vertical plate with uniform heat flux and mass transfer. Muthucumarswamy and Ganesan [16] investigated the transient natural convection flow of a viscous and incompressible fluid past an impulsively started vertical plate taking into account homogenous chemical reaction of first order. Another situation which frequently arises in chemical industries is MHD flow through a porous medium in the presence of chemical reaction. In one of the numerous porous media applications, such as in packed pebble bed-based blanket for fission-fusion hybrid reactors, to sustain a given flow rate of the electrically conducting liquid in the bed, the pressure drop and the liquid holdup will be increased under magnetohydrodynamic conditions compared with the case of non-conducting fluids.

Another application is in crystal growth where the use of external magnetic field has been successfully exploited to suppress unsteady flow and reduce non-uniform composition thereby enhancing quality of the crystal. Keeping in view the importance of such study, Singh and Kumar [17] studied the effects of chemical reaction on unsteady MHD heat and mass transfer flow past a hot vertical porous plate embedded in a porous medium in the presence of heat generation or absorption. Postelnicu [18] considered Soret and Dufour effects on natural convection heat and mass transfer flow over a vertical surface embedded in a fluid-saturated porous medium taking into account a homogenous chemical reaction of order n (where n was taken 1, 2, 3). Makinde [19] investigated MHD mixed-convection flow of an optically thin radiating fluid past a vertical porous plate embedded in a porous medium assuming n^{th} order homogenous chemical reaction between the fluid and the diffusing species. Pal and Talukdar [20] analyzed the effects of thermal radiation on unsteady hydromagnetic heat and mass transfer flow past a vertical moving plate embedded in a porous medium in the presence of heat absorption and first order chemical reaction of the species.

In all these investigations, analytical or numerical solution is obtained under different thermal conditions which are continuous and well defined. However, there are numerous practical problems which may require non-uniform or arbitrary thermal conditions. Pioneering work is due to Schetz [21] who developed an approximate model for free convection flow from a vertical plate with discontinuous thermal boundary conditions. Later on, Chandran *et al.* [22] analyzed the unsteady natural convective flow of a viscous and incompressible fluid near a vertical plate with ramped temperature. Patra *et al.* [23] considered the effects of radiation on the natural convection flow of a viscous and incompressible fluid near a stationary vertical flat plate with ramped temperature. Seth and Ansari [24] investigated the hydromagnetic natural convection flow past an impulsively moving vertical plate with ramped temperature in the presence of thermal diffusion and heat absorption. Seth *et al.* [25] also studied the effects of Hall current and rotation on the unsteady hydromagnetic natural convection flow of a viscous, incompressible, electrically conducting and heat absorbing fluid past an impulsively moving vertical plate with ramped temperature in a porous medium taking into account the effects of thermal diffusion. Nandkeolyar *et al.* [26] considered the unsteady hydromagnetic heat and mass transfer flow of a heat radiating fluid past a

flat porous plate with ramped wall temperature taking first order chemical reaction into account. Recently, Nandkeolyar *et al.* [27] presented an exact solution of unsteady MHD free convection heat and mass transfer flow of a heat absorbing fluid past a flat plate with ramped wall temperature.

In all above studies, induced magnetic field produced by the fluid motion is neglected in comparison to the applied one. This assumption is justified for metallic liquids and partially ionized fluids because magnetic Reynolds number is very small for metallic liquids and partially ionized fluids [28]. In contrast, for flows where magnetic Reynolds number is not very small, induced magnetic fields must be considered [29]. It is noticed that there are several astrophysical and geophysical problems in which induced magnetic field plays a vital role in determining flow features of the problem, namely, fluid flow in earth's interior, star formation, sunspots and solar flares in the Sun, rotating magnetic stars and planetary and solar dynamo problems. In addition to it, induced magnetic fields play a significant role in fusion applications with plasma containments [30] and on the performance of large scale pulsed MHD generators [31]. Moreover, induced magnetic fields could be used as an evidence to predict the existence of salty liquid-water subsurface oceans in Europa and Callisto [32]. The classical problem of Glauert [33] presented a seminal analysis for hydromagnetic boundary layer flow past a magnetized flat plate with uniform magnetic field in the stream direction at the plate. He obtained series of expansion solutions considering both large and small values of the electrical conductivity parameter for the velocity and induced magnetic fields. Raptis and Soundalgekar [34] investigated the flow of an electrically conducting fluid past a steadily moving infinite vertical porous plate in the presence of constant heat flux and constant suction taking induced magnetic field into account. Raptis and Masalas [35] considered the effects of induced magnetic field on the unsteady hydromagnetic flow of a viscous, incompressible, electrically conducting and optically thick radiating fluid past an infinite vertical porous plate. Bég *et al.* [36] obtained local non-similarity numerical solutions for the velocity, temperature and induced magnetic field distributions in forced convection liquid metal boundary layer flow past a non-conducting plate for a wide range of magnetic Prandtl numbers. Singh *et al.* [37] investigated the unsteady hydromagnetic natural convection flow between two insulated infinitely long vertical walls in the presence of induced magnetic field.

In view of the above analysis, the aim of the present study was to investigate the effects of induced magnetic field on the unsteady hydromagnetic natural convection heat and mass transfer flow of a viscous, incompressible, electrically conducting and heat absorbing fluid past an impulsively moving infinite vertical plate with ramped temperature embedded in a fluid-saturated porous medium in the presence of n^{th} order homogenous chemical reaction. To the best of our knowledge, no study has been reported in the literature by any researcher considering natural convection flow with heat and mass transfer of a chemically reacting fluid past a time dependent moving plate with ramped temperature taking induced magnetic field into account. The governing equations are solved using Crank-Nicolson implicit finite difference scheme. The numerical code is validated by comparing the values of the Nusselt number obtained through our present scheme with the earlier published results.

FORMULATION OF THE PROBLEM

Consider a unsteady hydromagnetic natural convection flow with heat and mass transfer of an electrically conducting, viscous, incompressible, chemically reacting and heat absorbing fluid past an infinite vertical plate embedded in a uniform porous medium in the presence of induced magnetic field. Coordinate system is chosen in such a way that x' - axis is considered along the plate in upward direction, y' - axis is perpendicular to the plane of the plate in the fluid and z' - axis is normal to the xy plane. A uniform transverse magnetic field B_0 is applied in a direction which is parallel to the y' - axis. Since induced magnetic field is taken into account, therefore the magnetic field $\vec{B} \equiv (B'_x, B_0, 0)$, where B'_x is the induced magnetic field in x' direction. Initially, i.e. at time $t' \leq 0$, both the fluid and the plate are at rest and are maintained at a uniform temperature T_∞' . Also species concentration within the fluid is maintained at a uniform value C_∞' . At time $t' > 0$, the plate starts moving in x' - direction with uniform velocity U_0 in its own plane. The temperature of the plate is raised or lowered to $T_\infty' + (T_w' - T_\infty')t'/t_0$ when $0 < t' \leq t_0$, and it is maintained at uniform temperature T_w' when $t' > t_0$ (t_0 being characteristic time). Also, at time $t' > 0$, species

concentration at the surface of the plate is raised to the uniform species concentration C_w' and is maintained thereafter. It is assumed that there exists a homogeneous chemical reaction of order n with constant rate K_2' between the diffusing species and the fluid.

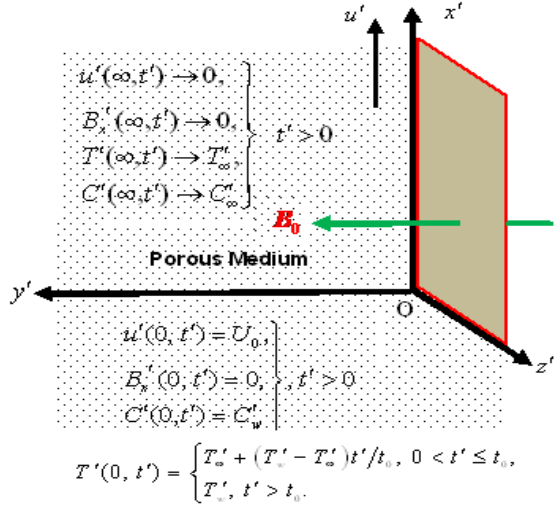


Fig. 1. Geometry of the problem.

Geometry of the problem is presented in Figure 1. Since the plate is of infinite extent in x' and z' directions and is electrically non-conducting, all physical quantities depend on y' and t' only.

Keeping in view the assumptions made above, the governing equations for MHD natural convection heat and mass transfer flow of an electrically conducting, viscous, incompressible and heat absorbing fluid through a uniform porous medium taking induced magnetic field and n^{th} order chemical reaction into account are given by

$$\frac{\partial u'}{\partial t'} = \nu \frac{\partial^2 u'}{\partial y'^2} + \frac{B_0}{\mu_e \rho} \frac{\partial B_x'}{\partial y'} - \frac{\nu u'}{K_1'} + g\beta'(T' - T_\infty') + g\beta^*(C' - C_\infty'), \quad (1)$$

$$\frac{\partial B_x'}{\partial t'} = \nu_m \frac{\partial^2 B_x'}{\partial y'^2} + B_0 \frac{\partial u'}{\partial y'}, \quad (2)$$

$$\frac{\partial T'}{\partial t'} = \frac{k}{\rho c_p} \frac{\partial^2 T'}{\partial y'^2} - \frac{Q_0}{\rho c_p} (T' - T_\infty'), \quad (3)$$

$$\frac{\partial C'}{\partial t'} = D \frac{\partial^2 C'}{\partial y'^2} - K_2' (C' - C_\infty')^n, \quad (4)$$

where u' , B_x' , T' , C' , c_p , D , g , k , K_1' , K_2' , Q_0 , β' , β^* , μ_e , ν , ρ , σ and $\nu_m = 1/\sigma\mu_e$ are fluid velocity in x' -direction, induced magnetic field in x' -direction, fluid temperature, species concentration,

specific heat at constant pressure, chemical molecular diffusivity, acceleration due to gravity, thermal conductivity of the fluid, permeability of the porous medium, chemical reaction coefficient, heat absorption coefficient, coefficient of thermal expansion, coefficient of expansion for species concentration, magnetic permeability, kinematic coefficient of viscosity, fluid density, electrical conductivity and magnetic diffusivity, respectively.

Initial and boundary conditions for the fluid flow problem are specified below:

$$u' = B_x' = 0, T' = T_\infty', C' = C_\infty' \text{ for } y' \geq 0 \text{ and } t' \leq 0, \quad (5a)$$

$$u' = U_0, B_x' = 0 \text{ at } y' = 0 \text{ for } t' > 0, \quad (5b)$$

$$T' = T_\infty' + (T_w' - T_\infty')t'/t_0 \text{ at } y' = 0 \text{ for } 0 < t' \leq t_0, \quad (5c)$$

$$T' = T_w' \text{ at } y' = 0 \text{ for } t' > t_0, \quad (5d)$$

$$C' = C_w' \text{ at } y' = 0 \text{ for } t' > 0, \quad (5e)$$

$$u', B_x' \rightarrow 0, T' \rightarrow T_\infty', C' \rightarrow C_\infty' \text{ as } y' \rightarrow \infty \text{ for } t' > 0. \quad (5f)$$

Equations (1) to (4), in non-dimensional form, assume the form:

$$\frac{\partial u}{\partial t} = \frac{\partial^2 u}{\partial y^2} + M^2 \frac{\partial B_x}{\partial y} - \frac{u}{K_1} + G_r T + G_c C, \quad (6)$$

$$P_m \frac{\partial B_x}{\partial t} = \frac{\partial^2 B_x}{\partial y^2} + \frac{\partial u}{\partial y}, \quad (7)$$

$$\frac{\partial T}{\partial t} = \frac{1}{P_r} \frac{\partial^2 T}{\partial y^2} - \phi T, \quad (8)$$

$$\frac{\partial C}{\partial t} = \frac{1}{S_c} \frac{\partial^2 C}{\partial y^2} - K_2 C^n, \quad (9)$$

where

$$y = y'/U_0 t_0, u = u'/U_0, B_x = B_x'/\sigma\mu_e \nu B_0, t = t'/t_0,$$

$$T = (T' - T_\infty')/(T_w' - T_\infty'), C = (C' - C_\infty')/(C_w' - C_\infty'),$$

$$G_r = g\beta' \nu (T_w' - T_\infty')/U_0^3, G_c = g\beta^* \nu (C_w' - C_\infty')/U_0^3,$$

$$M^2 = B_0^2 \sigma \nu / \rho U_0^2, K_1 = K_1' U_0^2 / \nu^2,$$

$$K_2 = K_2' (C_w' - C_\infty')^{n-1} t_0, P_m = \nu / \nu_m,$$

$$P_r = \nu \rho c_p / k, \phi = \nu Q_0 / \rho c_p U_0^2 \text{ and } S_c = \nu / D.$$

M^2 , K_1 , K_2 , G_r , G_c , P_m , P_r , ϕ and S_c are magnetic parameter, permeability parameter, chemical reaction parameter ([19]), thermal Grashof number, solutal Grashof number, magnetic Prandtl number, Prandtl number, heat absorption parameter and Schmidt number, respectively.

Characteristic time t_0 is defined according to the non-dimensional process mentioned above as $t_0 = \nu / U_0^2$.

Initial and boundary conditions (5a) to (5f), in non-dimensional form, become

$$u = 0, B_x = 0, T = 0, C = 0 \text{ for } y \geq 0 \text{ and } t \leq 0, \quad (10a)$$

$$u = 1, B_x = 0, \text{ at } y = 0 \text{ for } t > 0, \quad (10b)$$

$$T = t \text{ at } y = 0 \text{ for } 0 < t \leq 1, \quad (10c)$$

$$T = 1 \text{ at } y = 0 \text{ for } t > 1, \quad (10d)$$

$$C = 1 \text{ at } y = 0 \text{ for } t > 0, \quad (10e)$$

$$u \rightarrow 0, B_x \rightarrow 0, T \rightarrow 0, C \rightarrow 0 \\ \text{as } y \rightarrow \infty \text{ for } t > 0. \quad (10f)$$

NUMERICAL SOLUTION

Equations (6) to (9) cannot be solved analytically due to the coupled nature of equations (6) and (7) and the presence of a non-linear term in equation (9). Therefore, in order to understand the physical aspect of the problem, we have solved equations (6) to (9) under the initial and boundary conditions (10) by the Crank-Nicolson implicit finite difference scheme. The region under consideration was restricted by a rectangle of finite dimensions with $y_{\text{max}}=6$ (corresponding to $y \rightarrow \infty$) and $t_{\text{max}}=2$. Assumption of $y_{\text{max}} = 6$ was finalized when the boundary condition (10f) was satisfied within tolerance limit of 10^{-4} . The computational domain is divided into 241×801 grid points and the grid refinement check is performed by comparing the results in this case (with mesh size $\Delta y \times \Delta t$ where $\Delta y = 1/40$ and $\Delta t = 1/400$) with the results obtained when mesh size is reduced to 50% of the present case and it is noticed that the difference between these two results is less than half a unity in the fourth decimal place. The finite difference equations for each time step constitute a tridiagonal system of equations which are solved by Thomas algorithm as given in Carnahan *et al.* [38]. The numerical solution is then obtained corresponding to a desired time through iterations. It was found that the absolute difference between the numerical values of species concentration, fluid temperature, fluid velocity and induced magnetic field obtained for two consecutive time steps is less than 10^{-4} . Hence, the scheme designed is stable. Moreover, Crank-Nicolson method has a local truncation error of $O\{(\Delta y)^2 + (\Delta t)^2\}$ which tends to zero as Δy and Δt tends to zero which justifies consistency (Antia [39], pp. 643-644). Stability and consistency together ensure convergence of the scheme.

Now in order to highlight the effects of ramped temperature distribution within the plate on the flow-field, it is justified to compare such a flow

with the one past an impulsively moving vertical plate with uniform temperature. Taking into account the assumptions made in this paper, the numerical solutions for fluid temperature, fluid velocity and induced magnetic field for the flow past an impulsively moving isothermal vertical plate are obtained in the same manner as above and are displayed graphically along with the solutions obtained in case of ramped temperature plate for a better interpretation of the results.

Meanwhile, by using the computed values of fluid velocity and fluid temperature, the numerical values of skin friction τ and Nusselt number N_u for both ramped temperature and isothermal plates are obtained as follows:

$$\tau = \left. \frac{\partial u}{\partial y} \right|_{y=0}, \quad (11)$$

$$N_u = \left. \frac{\partial T}{\partial y} \right|_{y=0}. \quad (12)$$

The numerical values of Sherwood number S_h are also obtained as:

$$S_h = \left. \frac{\partial C}{\partial y} \right|_{y=0}. \quad (13)$$

The derivatives involved in equations (11) to (13) are evaluated using five point forward difference formula for the first derivative (Antia [39], page 161).

Validation of Numerical Solution

In order to validate our numerical scheme we have presented a comparison in Table 1 of the values of the Nusselt number obtained numerically from (12) with the values of the Nusselt number computed from the exact expression for Nusselt number obtained by Seth *et al.* [41] for various values of ϕ and t for both ramped temperature and isothermal plates taking $P_r = 0.71$. It is evident from Table 1 that the numerical values of the Nusselt number obtained through our numerical scheme are in very good agreement with the exact values of the Nusselt number obtained by Seth *et al.* [41]. This justifies the correctness of the results presented in the paper.

We have also made a comparison in Fig. 2 of the numerical values of species concentration obtained through our scheme with the exact solution presented by Khan *et al.* [42] taking $K_2 = 0$ (i.e. in absence of chemical reaction) in our model. It is observed that there is a very good agreement of the numerical solution with the exact solution.

Table 1. Nusselt number - N_u when $P_r = 0.71$

$t \rightarrow$ $\phi \downarrow$	For ramped temperature plate						For isothermal plate					
	Numerical values obtained by the present scheme			Exact values obtained by Seth <i>et al.</i> [41]			Numerical values obtained by the present scheme			Exact values obtained by Seth <i>et al.</i> [41]		
	0.3	0.5	0.7	0.3	0.5	0.7	0.3	0.5	0.7	0.3	0.5	0.7
1	0.5712	0.7789	0.9691	0.5713	0.7791	0.9693	1.1166	0.9834	0.9255	1.1160	0.9830	0.9253
3	0.6643	0.9666	1.2621	0.6645	0.9670	1.2624	1.5505	1.4881	1.4700	1.5500	1.4879	1.4700
5	0.7485	1.1287	1.5064	0.7490	1.1294	1.5070	1.9211	1.8914	1.8860	1.9209	1.8916	1.8860

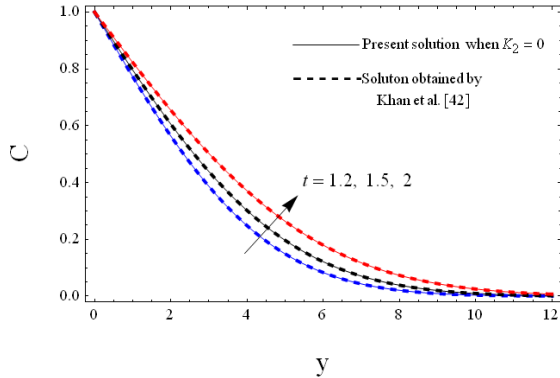


Fig. 2. Concentration profiles for different values of t when $S_c = 0.2$

RESULTS AND DISCUSSION

In order to analyze the effects of magnetic field, thermal buoyancy force, concentration buoyancy force, mass diffusion, chemical reaction, order of chemical reaction, heat absorption and time on the flow-field, the numerical solutions of fluid velocity $u(y,t)$ and induced magnetic field $B_x(y,t)$ in the boundary layer region are displayed graphically *versus* boundary layer coordinate y in Figs. 3 to 18 for various values of magnetic parameter M^2 , thermal Grashof number G_r , solutal Grashof number G_c , Schmidt number S_c , chemical reaction parameter K_2 , order n of chemical reaction, heat absorption parameter ϕ and time t taking $K_1 = 0.4$, $P_r = 0.71$ and $P_m = 0.7$ (ionized hydrogen) [40]. Figs. 3 to 18 reveal that for both

ramped temperature and isothermal plates, fluid velocity and induced magnetic field first increase to a distinctive maximum value and then decrease properly on increasing boundary layer coordinate y to approach free stream value. It is also noticed that fluid velocity is slower in the case of ramped temperature plate than in the case of isothermal plate. Moreover, induced magnetic field is higher in the case of isothermal plate than in the case of ramped temperature plate.

Figure 3 depicts the influence of magnetic field on fluid velocity u for both ramped temperature and isothermal plates. It is evident from Figure 3 that for both ramped temperature and isothermal plates, u decreases in the region near the plate on increasing M^2 while it increases in the region away from the plate on increasing M^2 . This implies that magnetic field tends to retard fluid velocity in the region near the plate whereas it has a reverse effect on fluid velocity in the region away from the plate. This shows that the Lorentz force (a resistive force developed due to the movement of an electrically conducting fluid in the presence of magnetic field) is dominant in the region near the plate and its effectiveness gets diminished by other forces in the region away from the plate. Figures 4 and 5 exhibit the effects of thermal and concentration buoyancy forces on fluid velocity for both ramped temperature and isothermal plates. Figs. 4 and 5 reveal that for both ramped temperature and isothermal

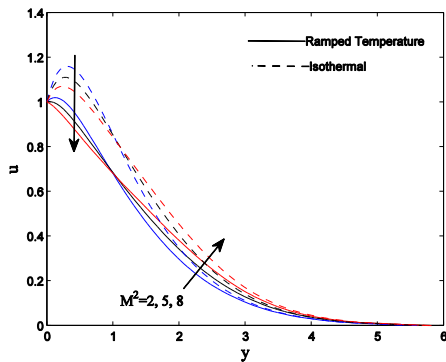


Fig. 3: Velocity profiles when $G_r = 5$, $G_c = 4$, $K_2 = 2.5$, $\phi = 3$, $n = 2$, $t = 0.5$ and $S_c = 0.22$

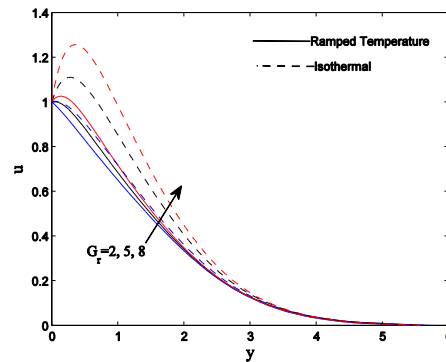


Fig. 4: Velocity profiles when $M^2 = 5$, $G_c = 4$, $K_2 = 2.5$, $\phi = 3$, $n = 2$, $t = 0.5$ and $S_c = 0.22$

plates, u increases on increasing G_r and G_c throughout the boundary layer region. Physically, G_r represents the relative strength of thermal buoyancy force to viscous force and G_c represents the relative strength of concentration buoyancy force to viscous force. Therefore, G_r and G_c increase on increasing the strengths of thermal and concentration buoyancy forces, respectively. In this problem a natural convection flow is induced due to thermal and concentration buoyancy forces, therefore thermal and concentration buoyancy forces tend to accelerate fluid velocity for both ramped temperature and isothermal plates throughout the boundary layer region.

Figures 6 and 7 demonstrate the effects of rate of chemical reaction and heat absorption on fluid

velocity for both ramped temperature and isothermal plates. It is perceived from Figs. 6 and 7 that u decreases on increasing K_2 and ϕ for both ramped temperature and isothermal plates throughout the boundary layer region. This implies that for both ramped temperature and isothermal plates, chemical reaction and heat absorption tend to retard fluid velocity, which is due to the fact that chemical reaction and heat absorption inhibit concentration and thermal buoyancy forces, respectively. Figures 8 and 9 display the influence of the order of chemical reaction and time on fluid velocity for both ramped temperature and isothermal plates. It is depicted in Figs. 8 and 9 that u increases on increasing n and t for

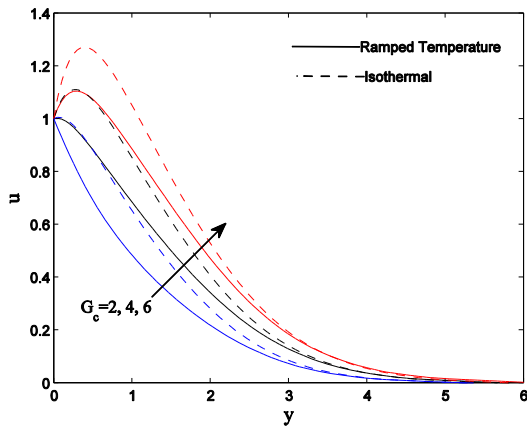


Fig. 5: Velocity profiles when $M^2 = 5$, $G_r = 5$, $K_2 = 2.5$, $\phi = 3$, $n = 2$, $t = 0.5$ and $S_c = 0.22$

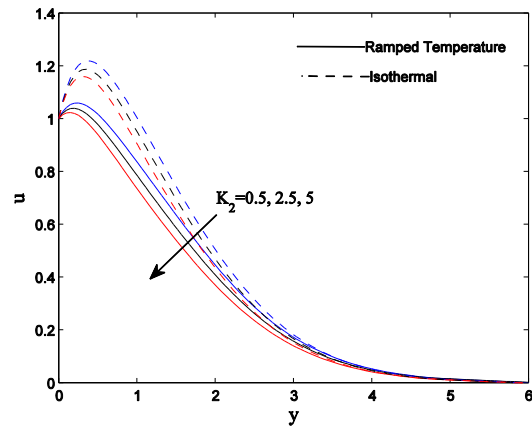


Fig. 6: Velocity profiles when $M^2 = 5$, $G_r = 5$, $G_c = 4$, $\phi = 3$, $n = 2$, $t = 0.5$ and $S_c = 0.22$

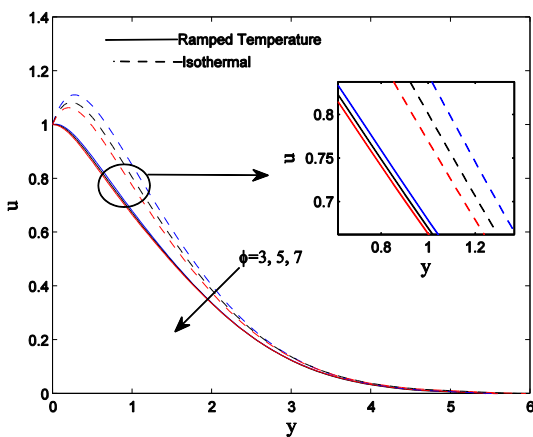


Fig. 7: Velocity profiles when $M^2 = 5$, $G_r = 5$, $G_c = 4$, $K_2 = 2.5$, $n = 2$, $t = 0.5$ and $S_c = 0.22$

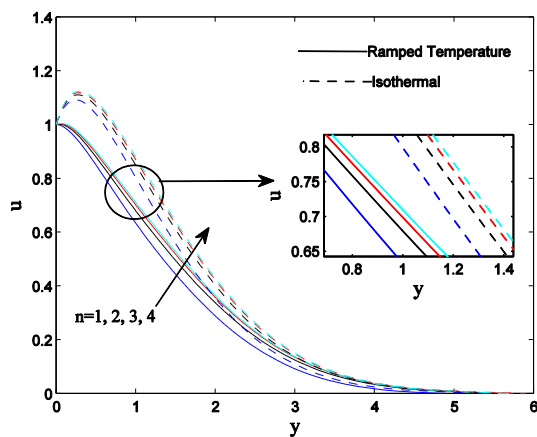


Fig. 8: Velocity profiles when $M^2 = 5$, $G_r = 5$, $G_c = 4$, $K_2 = 2.5$, $\phi = 3$, $t = 0.5$ and $S_c = 0.22$

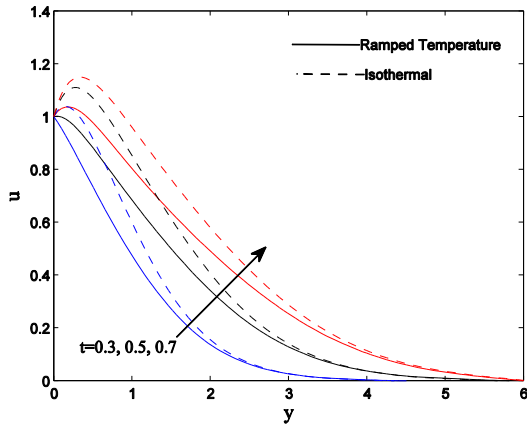


Fig. 9: Velocity profiles when $M^2 = 5$, $G_r = 5$, $G_c = 4$, $K_2 = 2.5$, $\phi = 3$, $n = 2$ and $S_c = 0.22$

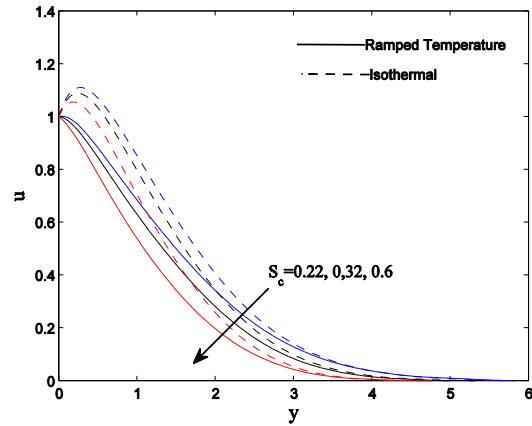


Fig. 10: Velocity profiles when $M^2 = 5$, $G_r = 5$, $G_c = 4$, $K_2 = 2.5$, $\phi = 3$, $n = 2$ and $t = 0.5$

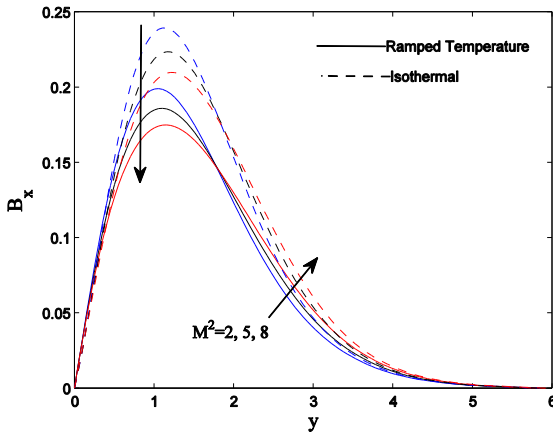


Fig. 11: Induced magnetic field profiles when $G_r = 5$, $G_c = 4$, $K_2 = 2.5$, $\phi = 3$, $n = 2$, $t = 0.5$ and $S_c = 0.22$

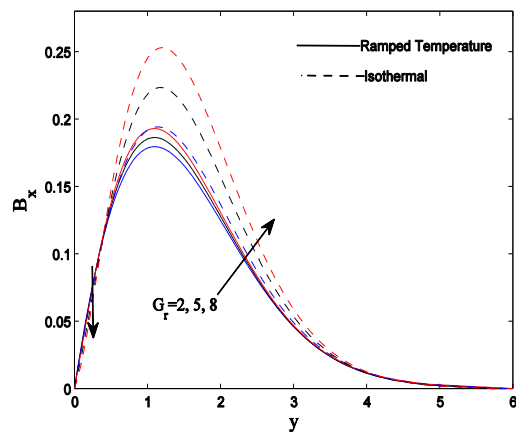


Fig. 12: Induced magnetic field profiles when $M^2 = 5$, $G_c = 4$, $K_2 = 2.5$, $\phi = 3$, $n = 2$, $t = 0.5$ and $S_c = 0.22$

both ramped temperature and isothermal plates throughout the boundary layer region. This implies that for both ramped temperature and isothermal plates, the order of the chemical reaction tends to accelerate fluid velocity but the increment almost dies out after a certain level. For both ramped temperature and isothermal plates, fluid velocity is getting accelerated with the progress of time. Figure 10 portrays the effects of mass diffusion on fluid velocity for both ramped temperature and isothermal plates. It is evident from Figure 10 that u decreases on increasing S_c for both ramped temperature and isothermal plates throughout the boundary layer region. Since Schmidt number S_c is a measure of the relative strength of viscosity to molecular (mass) diffusivity of the fluid, S_c decreases on increasing molecular diffusivity

of the fluid. This implies that mass diffusion tends to accelerate fluid velocity for both ramped temperature and isothermal plates. Figure 11 demonstrates the effects of magnetic field on induced magnetic field for both ramped temperature and isothermal plates. It is apparent from Figure 11 that B_x decreases on increasing M^2 in the region near the plate while it increases on increasing M^2 in the region away from the plate for both ramped temperature and isothermal plates. This implies that externally applied magnetic field tends to reduce induced magnetic field in the region near the plate whereas it has a reverse effect on induced magnetic field in the region away from the plate. Figures 12 and 13 illustrate the effects of thermal and concentration buoyancy forces on the induced magnetic field for both ramped temperature and isothermal plates.

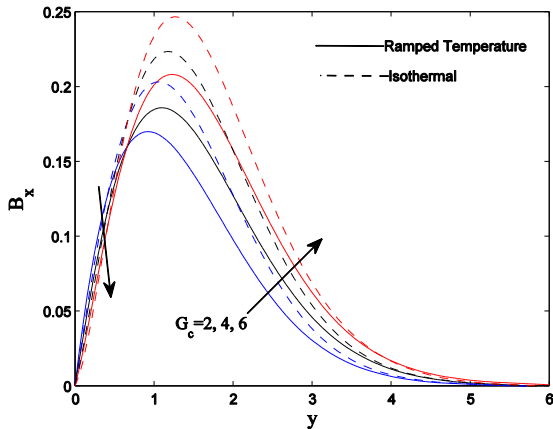


Fig. 13: Induced magnetic field profiles when $M^2 = 5$, $G_r = 5$, $K_2 = 2.5$, $\phi = 3$, $n = 2$, $t = 0.5$ and $S_c = 0.22$

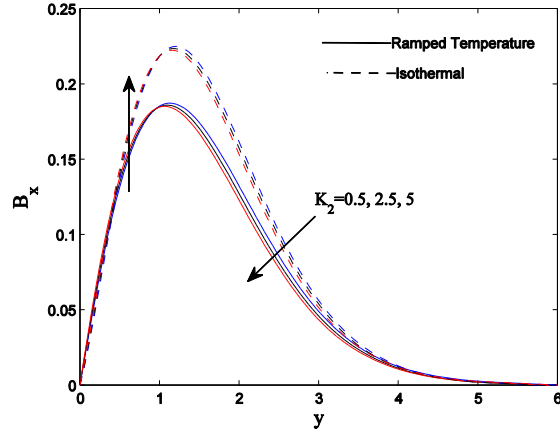


Fig. 14: Induced magnetic field profiles when $M^2 = 5$, $G_r = 5$, $G_c = 4$, $\phi = 3$, $n = 2$, $t = 0.5$ and $S_c = 0.22$

It is seen from Figs. 12 and 13 that B_x decreases on increasing G_r and G_c in the region near the plate while it increases on increasing G_r and G_c in the region away from the plate for both ramped temperature and isothermal plates. This implies that thermal and concentration buoyancy forces tend to reduce induced magnetic field in the region near the plate while they have reverse effect on the induced magnetic field in the region away from the plate. Figures 14 to 16 depict the effects of chemical reaction, heat absorption and mass diffusion on the induced magnetic field

for both ramped temperature and isothermal plates. It is perceived from Figs. 14 to 16 that B_x increases on increasing K_2 , ϕ and S_c in the region near the plate while it decreases on increasing K_2 , ϕ and S_c in the region away from the plate. This implies that chemical reaction and heat absorption tend to enhance the induced magnetic field in the region near the plate while they have reverse effect on the induced magnetic field in the region away from the plate. Mass diffusion tends to reduce the induced magnetic field in the region near the plate while it has a reverse effect on the induced magnetic field in the region away from the plate.

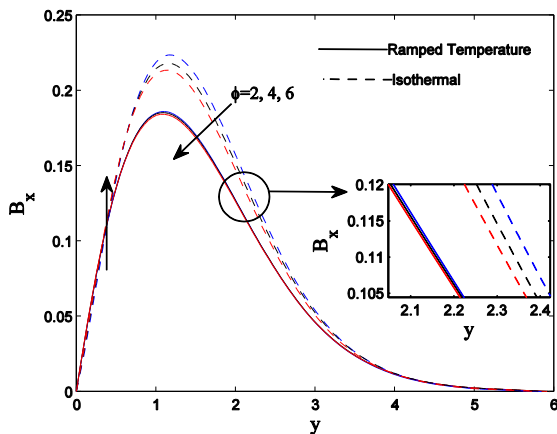


Fig. 15: Induced magnetic field profiles when $M^2 = 5$, $G_r = 5$, $G_c = 4$, $K_2 = 2.5$, $n = 2$, $t = 0.5$ and $S_c = 0.22$

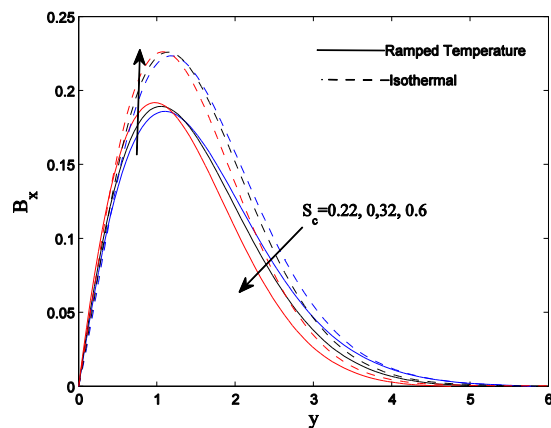


Fig. 16: Induced magnetic field profiles when $M^2 = 5$, $G_r = 5$, $G_c = 4$, $K_2 = 2.5$, $n = 2$, $t = 0.5$ and $\phi = 3$

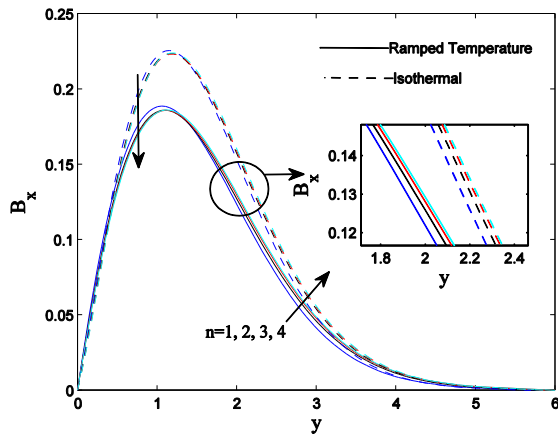


Fig. 17: Induced magnetic field profiles when $M^2 = 5, G_r = 5, G_c = 4, K_2 = 2.5, \phi = 3, t = 0.5$ and $S_c = 0.22$

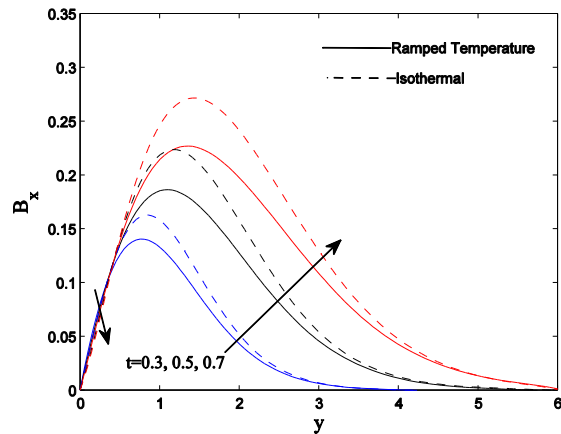


Fig. 18: Induced magnetic field profiles when $M^2 = 5, G_r = 5, G_c = 4, K_2 = 2.5, n = 2, \phi = 3$ and $S_c = 0.22$

Figures 17 and 18 portray the influence of the order of chemical reaction and time on the induced magnetic field for both ramped temperature and isothermal plates. It is observed from Figs. 17 and 18 that B_x decreases on increasing n and t in a close proximity to the plate while it increases on increasing n and t in the region just away from the plate. This implies that the order of chemical reaction reduces the induced magnetic field in the region near the plate whereas it has a reverse effect on the induced magnetic field in the region away from the plate. Induced magnetic field is getting enhanced with the progress of time in most of the region of the plate.

In order to study the effects of chemical reaction, order of chemical reaction and mass diffusion on species concentration, the numerical

solutions of species concentration C , are presented graphically *versus* boundary layer coordinate y in Figs. 19 to 21 for various values of chemical reaction parameter K_2 , order of chemical reaction n and Schmidt number S_c . It is observed from Figs. 19 to 21 that species concentration attains a distinctive maximum value near the surface of the plate and then decreases properly on increasing boundary layer coordinate y to approach the free stream value. It is evident from Figs. 19 to 21 that species concentration C decreases on increasing either K_2 or S_c while it increases on increasing n . This implies that chemical reaction tends to reduce species concentration whereas mass diffusion has a reverse effect on it. The order of the chemical reaction tends to enhance the species concentration but the incremental effect almost dies out after a certain level.

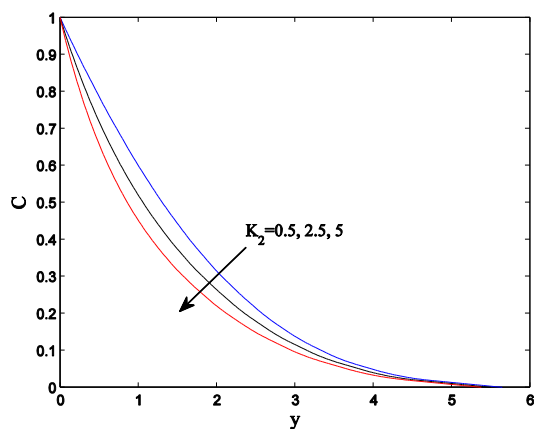


Fig. 19: Concentration profiles when $n = 2, t = 0.5$ and $S_c = 0.22$

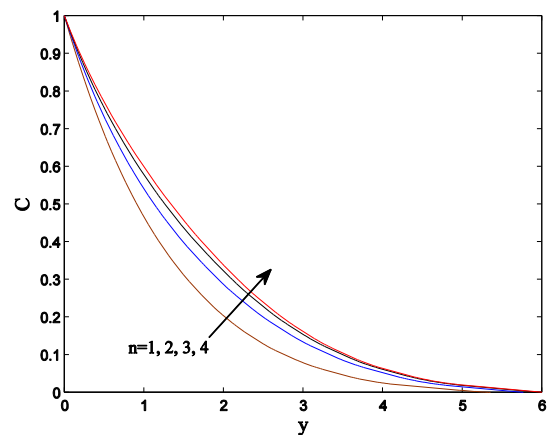


Fig. 20: Concentration profiles when $K_2 = 2.5, t = 0.5$ and $S_c = 0.22$

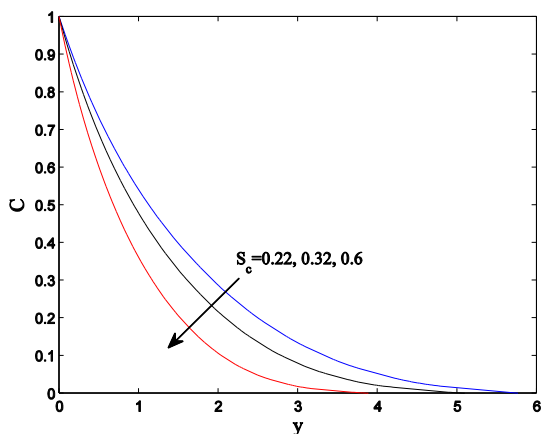


Fig. 21: Concentration profiles when $K_2 = 2.5, t = 0.5$ and $n = 2$

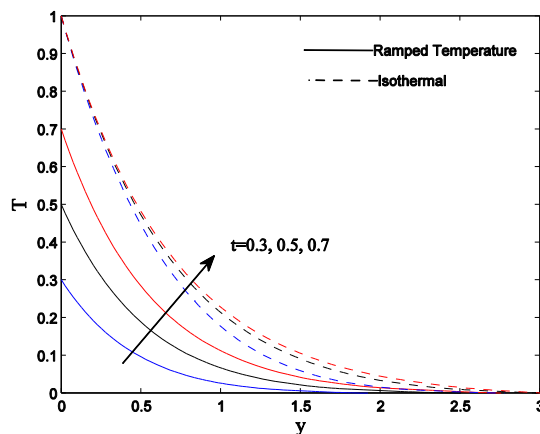


Fig. 22: Temperature profiles when $P_r = 0.71$ and $\phi = 3$

Figure 22 presents the influence of time on fluid temperature T for both ramped temperature and isothermal plates. It is evident from Fig. 22 that T increases on increasing t for both ramped temperature and isothermal plates. This implies that fluid temperature increases with the progress of time for both ramped temperature and isothermal plates.

Skin friction

Numerical values of skin friction τ , for both ramped temperature and isothermal plates, are computed from (11) and are presented in tabular form in Tables 2 and 3 for various values of $M^2, G_r, G_c, S_c, K_2, n, \phi$ and t taking $P_r = 0.71, P_m = 0.7$ [40] and $K_1 = 0.4$. It is observed from Table 2 that for both ramped temperature and isothermal plates, τ increases on increasing M^2, S_c and ϕ . This implies that magnetic field and heat absorption tend to enhance

skin friction whereas mass diffusion has a reverse effect on it. It is also noticed from Table 2 that τ decreases, attains a minimum and then increases on increasing t for both ramped temperature and isothermal plates. It is evident from Table 3 that on increasing G_r, τ decreases for ramped temperature plate and it decreases, attains a minimum and then increases for isothermal plate. τ increases on increasing G_c and n whereas it decreases on increasing K_2 for both ramped temperature and isothermal plates. This implies that thermal buoyancy force tends to reduce skin friction for ramped temperature plate. For both ramped temperature and isothermal plates, the order of the chemical reaction and the concentration buoyancy force tend to enhance skin friction whereas the rate of chemical reaction has a reverse effect on it. It is interesting to note from Tables 2 and 3 that there exists a separation of flow at the plate on increasing either G_r or G_c or t for both ramped temperature and isothermal plates.

Table 2. Skin friction $-\tau$ at ramped temperature and isothermal plates when $G_r = 5, G_c = 4, K_2 = 2.5$ and $n = 2$

M^2	S_c	ϕ	t	Ramped Temperature Plate	Isothermal Plate
2	0.22	3	0.1	1.4009	0.6135
5	0.22	3	0.1	1.5084	0.7261
8	0.22	3	0.1	1.6229	0.8455
5	0.32	3	0.1	1.5626	0.7803
5	0.6	3	0.1	1.6683	0.8860
5	0.6	5	0.1	1.6692	0.9065
5	0.6	7	0.1	1.6701	0.9259
5	0.22	3	0.3	0.4172	-0.5725
5	0.22	3	0.5	-0.0814	-0.9503
5	0.22	3	0.7	-0.4600	-1.0960

Table 3. Skin friction $-\tau$ at ramped temperature and isothermal plates when $M^2 = 5$, $S_c = 0.22$, $\phi = 3$ and $t = 0.5$

G_r	G_c	K_2	n	Ramped Temperature Plate	Isothermal Plate
2	2	0.5	2	1.0021	0.6545
5	2	0.5	2	0.6698	-0.1992
8	2	0.5	2	0.3374	-1.0529
5	4	0.5	2	-0.1708	-1.0397
5	6	0.5	2	-1.0113	-1.8803
5	4	2.5	2	-0.0814	-0.9503
5	4	2.5	3	-0.1175	-0.9864
5	4	2.5	4	-0.1380	-1.0069

Table 4: Sherwood number S_h

t	K_2	S_c	n	$-S_h$
0.1	0.5	0.22	2	0.9795
0.3	0.5	0.22	2	0.5377
0.5	0.5	0.22	2	0.4413
0.5	2.5	0.22	2	0.6619
0.5	2.5	0.32	2	0.7978
0.5	2.5	0.6	2	1.0923
0.5	2.5	0.6	3	1.0004
0.5	2.5	0.6	4	0.9411
0.5	5	0.6	4	1.1960

Sherwood number

Numerical values of Sherwood number which represents the rate of mass transfer at the plate are computed from (13) and are presented in Table 4 for various values of t , K_2 , S_c and n . It is perceived from Table 4 that S_h decreases on increasing t and n whereas it increases on increasing S_c and K_2 . This implies that chemical reaction tends to enhance the rate of mass transfer at the plate whereas mass diffusion and order of chemical reaction have reverse effect on it. The rate of mass transfer at the plate is getting reduced with the progress of time.

CONCLUSION

The present study analyses the effects of induced magnetic field on the unsteady hydromagnetic natural convection heat and mass transfer flow of a viscous, incompressible, electrically conducting and heat absorbing fluid past an impulsively moving infinite vertical plate with ramped temperature embedded in a fluid-saturated porous medium in the presence of n^{th} order homogenous chemical reaction. Significant results are summarized below:

For both ramped temperature and isothermal plates:

Magnetic field tends to retard fluid velocity in the region near the plate whereas it has a reverse

effect on fluid velocity in the region away from the plate.

Throughout the boundary layer region, thermal buoyancy force, concentration buoyancy force, mass diffusion and order of chemical reaction tend to accelerate fluid velocity whereas rate of chemical reaction and heat absorption have reverse effect on it. Fluid velocity is getting accelerated with the progress of time.

Externally applied magnetic field tends to reduce induced magnetic field in the region near the plate whereas it has a reverse effect on induced magnetic field in the region away from the plate.

Thermal buoyancy force, concentration buoyancy force, mass diffusion and order of chemical reaction tend to reduce induced magnetic field in the region near the plate while they have reverse effect on induced magnetic field in the region away from the plate.

Chemical reaction and heat absorption tend to enhance induced magnetic field in the region near the plate while they have reverse effect on induced magnetic field in the region away from the plate.

Magnetic field and heat absorption tend to enhance skin friction whereas mass diffusion has a reverse effect on it. Order of chemical reaction and concentration buoyancy force tend to enhance skin friction whereas rate of chemical reaction has a reverse effect on it. There exists a separation of flow at the plate on increasing either thermal buoyancy force or concentration buoyancy force or with the progress of time.

Acknowledgements: Authors are grateful to the reviewers for their valuable comments and suggestions which helped them to improve the quality of the research paper.

REFERENCES

1. E. R. Eckert, R. M. Drake, Analysis of Heat and Mass Transfer, Mc-Graw Hill, New York, 1972.
2. A. Bejan, K. R. Khair, *Int. J. Heat Mass Transf.*, **28**, 909 (1985).
3. J. Y. Jang, W. J. Chang, *Int. Commun. Heat Mass Transf.*, **15**, 17 (1988).
4. F. C. Lai, F. A. Kulacki, *J. Heat Transf.*, **113**, 252 (1991).
5. A. Nakayama, M. A. Hossain, *Int. J. Heat Mass Transf.*, **38**, 761 (1995).
6. M. A. Hossain, A. C. Mandal, *J. Phys. D: Appl. Phys.*, **18**, 163 (1985).
7. B. K. Jha, *Astrophysics Space Sci.*, **175**, 283 (1991).
8. F. S. Ibrahim, I. A. Hassanien, A. A. Bakr, *Canad. J. Phys.*, **82**, 775 (2004).
9. K. Das, S. Jana, *Bull. Soc. Math. Banja Luka*, **17**, 15 (2010).
10. N. T. M. Eldabe, E. M. A. Elbashbeshy, W. S. A. Hasanin, E. M. Elsaid, *Int. J. Energy Tech.* **3**, 1 (2011).
11. A. J. Chamkha, A. A. Khaled, *Int. J. Numer. Methods Heat Fluid Flow*, **10**, 455 (2000).
12. M. H. Kamel, *Energy Conv. Management*, **42**, 393 (2001).
13. A. J. Chamkha, *Int. J. Engng. Sci.*, **42**, 217 (2004).
14. P. L. Chambré, J. D. Young, *Phys. Fluids*, **1**, 48 (1958).
15. U. N. Das, R. K. Deka, V. M, Soundalgekar, *Forschung im Ingenieurwesen*, **60**, 284 (1994).
16. R. Muthucumarswamy, P, Ganesan, *Forschung im Ingenieurwesen*, **66**, 17 (2000).
17. K. D. Singh, R. Kumar, *Indian J. Phys.*, **84**, 93 (2010).
18. A. Postelnicu, *Heat Mass Transf.*, **43**, 595 (2007).
19. O. D. Makinde, *Chem. Eng. Comm.*, **198**, 590 (2010).
20. D. Pal, B. Talukdar, *Math. Computer Modelling*, **54**, 3016 (2011).
21. J. A. Schetz, *J. Appl. Mech.*, **30**, 263 (1963).
22. P. Chandran, N. C. Sacheti, A. K. Singh, *Heat Mass Transf.*, **41**, 459 (2005).
23. R. R. Patra, S. Das, R. N. Jana, S. K. Ghosh, *J. Appl. Fluid Mech.*, **5**, 9 (2012).
24. G. S. Seth, Md. S. Ansari, *Int. J. Appl. Mech. Eng.*, **15**, 199 (2010).
25. G. S. Seth, G. K. Mahato, S. Sarkar, *Int. J. Energy Tech.*, **5**, 1 (2013).
26. R. Nandkeolyar, M. Das, P. Sibanda, *Math. Problems Eng.* **2013** Article ID 381806 (2013).
27. R. Nandkeolyar, M. Das, P. Sibanda, *Boundary Value Problems*, **2013**, 247 (2013).
28. K. R. Cramer, S. I. Pai, Magnetofluid dynamics for engineers and applied physicists, New York: McGraw Hill, 1973.
29. A. Pantokratoras, *J. Appl. Phys.*, **102**, 076113 (2007).
30. K. Takenouchi, *J. Phys. Soc. Japan*, **54**, 1329 (1985).
31. Y. Koshiha, T. Matsushita, M. Ishikawa *Influence of induced magnetic field on large-scale pulsed MHD generator*, in: AIAA 33rd Plasmadynamics and Lasers Conference, Maui, Hawaii, May 20-23, 2002.
32. K. K. Khurana, M. G. Kivelson, D. J. Stevenson, G. Schubert, C. T. Russell, R. J. Walker, C. Polanskey, *Nature*, **395**, 777 (1998).
33. M. B. Glauert, *J. Fluid Mech.* **10**, 276 (1961).
34. A. Raptis, V. Soundalgekar, *Nuclear Eng. Des.*, **72**(3), 373 (1982).
35. A. Raptis, C. V. Massalas, *Heat Mass Transf.*, **34**, 107 (1998).
36. O. A. Beg, A. Y. Bakier, V. R. Prasad, J. Zueco, S. K. Ghosh, *Int. J. Thermal Sci.*, **48**, 1596 (2009).
37. R. K. Singh, A. K. Singh, N. C. Sacheti, P. Chandran, *Heat Mass Transf.*, **46**, 523 (2010).
38. B. Carnahan, H. A. Luther, J. O. Wilkes, Applied Numerical Methods, New York, John Wiley, 1969.
39. H. M. Antia, Numerical Methods for Scientists and Engineers, New Delhi: Tata McGraw-Hill Publishing Co Ltd, 1991.
40. E. R. Benton, D. E. Loper, *J. Fluid Mech.*, **39**, 561 (1969).
41. G. S. Seth, S. M. Hussain, S. Sarkar, *J. Egyptian Math. Soc.*, **23**, 197 (2015).
42. A. Khan, I. Khan, F. Ali, Samiulhaq, S. Shafie, *Plos One*, **9**(3): e90280. doi:10.1371/journal.pone (2014).

ТЕЧЕНИЕ С ЕСТЕСТВЕНА КОНВЕКЦИЯ В ИНДУЦИРАНО МАГНИТНО ПОЛЕ И ХИМИЧНА РЕАКЦИЯ ОТ n -ТИ ПОРЯДЪК, СЪПРОВОДЕНА С ПОГЛЪЩАНЕ НА ТОПЛИНА ОТ ДВИЖЕЩА СЕ ПЛОСКОСТ С ТЕМПЕРАТУРЕН ПРОФИЛ

Г.С. Сет*, С. Саркар

Департамент по приложна математика, Индийско минно училище, Дханбад 826004, Индия

Постъпила на 3 януари, 2014 г. коригирана на 26 август, 2014 г.

(Резюме)

Изследвано е течение под действие на естествена конвекция в нестационарно магнитно поле, съпроводено от топло- и масопренасяне във вискозен, електропроводящ и топло-поглъщащ флуид зад подвижна вертикална плоскост с температурен профил. Отчетен е ефектът на химична реакция от n -ти порядък. Уравненията на движението и на преноса са решени с използването на крайна диференчна схема по Crank-Nicolson. Численото решение за разпределението на скоростите, индуцираното магнитно поле, концентрациите на веществата и температурата на флуида са представено графично, а стойностите на коефициента на триене и числата на Sherwood и Nusselt са дадени в табличен вид. Влиянието на температурния профил на стената върху течението е сравнено със случая на изотермична стена. Коректността на числените резултати е потвърдена.